THE SPECTROSCOPY OF FISSION FRAGMENTS * **

W.R. PHILLIPS

Department of Physics and Astronomy, University of Manchester
Manchester, M13 9PL, U.K.

(Received December 10, 1996)

High-resolution measurements on γ rays from fission fragments have given a wealth of information on neutron-rich nuclei and on the mechanism of the fission process. In recent years important data have been obtained on the yrast and near-yrast structures of neutron-rich nuclei with up to ten more neutrons than the nearest stable isotope. This paper discusses the scope of measurements which can be made on prompt gamma rays from spontaneous fission fragments, the techniques used in the experiments and some results recently obtained.

PACS numbers: 23.20. -g, 23.20. En, 23.20. Lv, 27.60. +j

1. Introduction

Experiments made to study neutron-rich nuclei with as large a neutron excess as possible are performed on fragments produced in low-energy fission such as spontaneous fission or fission induced by low-energy neutron or proton beams. This paper is concerned with experiments on fragments formed in spontaneous fission, such as of ^{252}Cf or ^{248}Cm. These sources give rise to the characteristic double-humped mass distribution. The prompt-gamma emitting species amenable to study are determined by the atomic number distribution for a given mass and by the power of the gamma-ray detection array used in the experiments. Results discussed here were obtained using the EUROGAM array, and the techniques outlined were designed for use with that array although applicable to any similar detection equipment. This paper first discusses the scope of present measurements on spontaneous fission fragments showing the nuclei studied and the spin range

* Presented at the XXXI Zakopane School of Physics, Zakopane, Poland, September 3–11, 1996.

** Work supported by the Science and Engineering Research Council of the UK under grant no. GRH71161, and by the US Dept. of Energy under contract No. W-31-109-ENG-38.

over which discrete levels in these nuclei have been observed. Following that, the techniques used to obtain level schemes, level lifetimes, identify new nuclei and obtain gamma-ray correlation and polarization data are outlined. Finally some recent results obtained with EUROGAM2 are presented.

2. Mass, charge and spin distributions

The nuclei which can be studied via fission γ rays, and the spins of observable discrete levels, are determined by the range of secondary fragments made in realizable fissioning systems and by the range of spins the fission mechanism produces in the secondary fragments. Yields of fission products depend on the mass and charge of the nucleus which fissions and on its excitation energy. In general, fission of the ground state of a nucleus with a large N/Z ratio produces the most neutron-rich nuclei. Spontaneous fission and thermal-neutron induced fission have asymmetric mass distributions centred close to mass 100 and mass 140. It has been found that the mean mass of the higher mass peak remains the same for low energy fission of actinide nuclei of different mass but the mean mass of the lower peak increases with increase in mass of the fissioning nucleus. Thus, as shown in Fig. 1, yields of some of the nuclei produced in the thermal neutron induced fission of ^{235}U [1] are different from their yields in the spontaneous fission of ^{252}Cf [2].

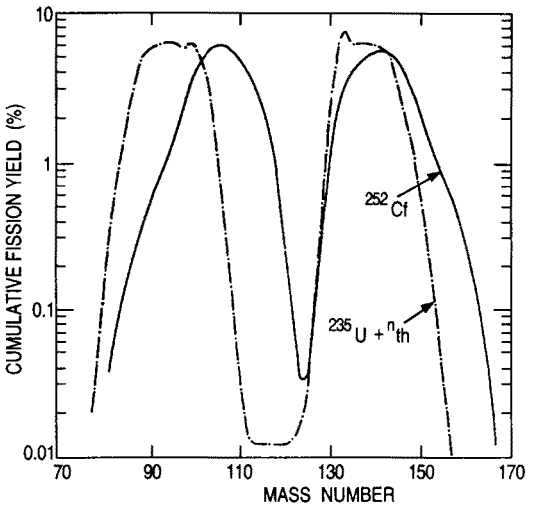

Fig. 1. Mass distributions in the spontaneous fission of ^{252}Cf and in the thermal-neutron induced fission of ^{235}U.

For a given mass number $A = (N + Z)$ of a secondary, prompt γ-emitting fragment, the most probable atomic number $Z_P(A)$ is given to a first approximation by

$$Z_P(A) = \frac{Z_f}{(A_f - \nu)} \times A\,,$$

where the subscript f refers to the fissioning nucleus and ν is the average number of neutrons emitted per fission. The charge distribution for a given A is given, to a good approximation, by

$$P(A, Z) = \sigma_Z (2\pi)^{1/2} \exp\left[-\frac{(Z_P(A) - Z)^2}{2\sigma_Z^2}\right],$$

where σ_Z the dispersion is close to 0.5.

For a given atomic number of the secondary fragment the mass number distribution is also given by an expression of the above form with the mass dispersion σ_A about equal to $0.5 \times (A_f/Z_f)$.

The spin distributions in fission fragments, together with the sensitivity of the detection equipment, determine the range of spins over which level structures in the fragments can be observed. The average spin in spontaneous fission fragments was known from early experiments [3, 4] to be in the range 6–7 $\hbar$. However, there is evidence that the spin distribution is skewed towards the high-spin side, and with the latest generation of γ-ray detector arrays it is possible to examine levels in strongly populated secondary fragments with spins up to $\sim 20\ \hbar$.

Normally fragments are formed hot at scission. A typical primary fragment may have an excitation energy of ~ 20 MeV and a spin of $\sim 7\ \hbar$. It cools down with emission of two neutrons leaving a secondary fragment at excitation energy of a few MeV. The secondary fragment then continues to deexcite by γ-ray emission. The γ rays in the secondary fragment arise from a broad range of excitation energy corresponding to the spread in energies of the neutrons emitted from the primary fragment. They also arise from levels with a large spread of spins corresponding to the spread in the primary fragments introduced by the fission mechanism. There are also many γ-ray paths to the ground state from any point in this entry region. A variable number of *statistical* γ rays, with essentially continuous energy distribution and relatively high energies of an MeV or greater, takes the secondary fragment from the initial chaotic entry region down to a more ordered regime in which there are rather few yrast or near-yrast levels. This is illustrated schematically in Fig. 2. The number of statistical γ rays depends partly on the initial excitation energy of the primary fragment; in spontaneous fission there are typically one to three statistical γ rays per fragment.

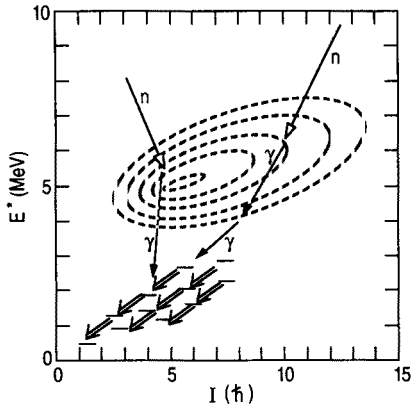

Fig. 2. Schematic diagram showing entry points into a prompt γ-ray emitting fragment after neutron evaporation from a hot primary fragment formed at scission.

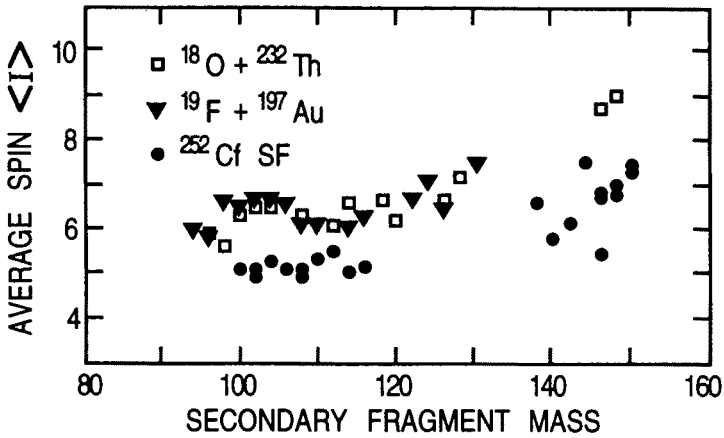

Fig. 3. Average spins at which discrete levels are populated in prompt γ-ray emitting fragments formed in the spontaneous fission of ^{252}Cf, the fission of ^{232}Th with 120 MeV ^{18}O ions and the fission of ^{197}Au with 120 MeV ^{19}F ions.

Fig. 3 shows the average spins $\langle I \rangle$ of formation of discrete levels in fragments from three different fission processes. The data were obtained from direct analyses of the intensities of the discrete γ rays using the procedure outlined in Ref. [5]. The figure shows that heavy-ion induced fusion-fission gives higher values of $\langle I \rangle$ than low-energy fission, and should therefore allow the construction of level schemes up to higher spins. However, this advantage is outweighed by the disadvantages that *(i)* the mass distributions are

broadened, making it experimentally more difficult to examine in detail any one product, and *(ii)* the fragments are on average less neutron-rich than in low energy fission because more neutrons are emitted in total as pre-fission neutrons and/or from the more highly excited primary fragments.

3. Experimental techniques

The chief difficulty when performing experiments on prompt γ rays from fission products is that many pairs of fragments are formed, each one typically emitting several γ-rays. A particular nucleus under investigation needs a high degree of selectivity, and in prompt γ-ray experiments this is obtained by demanding time coincidences between (usually) three or more γ-rays from the same fission event. Fragments come in pairs, and greater than 99% of pairs have $Z_1 + Z_2$ equal to Z_f. Gating on a known γ ray in a particular nucleus (A_1, Z_1) gives rise to coincident lines in several nuclei since there is a range of mass numbers A_2 accompanying Z_2. Although this complicates coincidence spectra, it can sometimes be helpful since it enables spectra containing (apart from impurities) only lines in two nuclei to be produced.

The usual techniques of γ-ray analysis are used to determine partial decay schemes in fragments. Triple coincidences are organized into three-dimensional arrays, each axis corresponding to energies deposited in a germanium detector. Gating on two axes enables spectra of coincident γ rays to be produced and used to build up decay patterns. The starting points are usually lines known from earlier work, often studies of mass isolated beta-decaying fission product ground states. When nuclei about which nothing was previously known have been examined their identification has been made by comparing the yields of complementary fragments; the average complementary fragment mass is a good signature of the mass of the new fragment studied [6, 7].

The nearly 4π coverage of EUROGAM2 and the close arrangement of four individual germanium crystals in the 'clover' detectors used in that array have allowed the application of γ-ray correlation and polarization techniques to greatly increase the spectroscopic information obtained on fission fragments.

4. Directional correlations

When prompt γ rays are observed in an array without observation of fragments, the first γ ray in a decay sequence arises from the decay of a state which is unaligned, *i.e.* equally populated amongst its magnetic substates. For a cascade of two γ rays the second is then distributed anisotropically

with respect to the first and if the directional correlation is measured information can be obtained on the spins of the levels involved in the transitions and on the multipolarities of the two γ rays. Measurements on double cascades as described above are of limited use because of the lack of selectivity when using only a single coincidence gate on a fission spectrum. A second gate on the second axis of a three-dimensional data array (cube) is required in order to increase the resolving power. However, if the first axis of a cube containing triple coincidences corresponds to γ rays observed anywhere in the array while the other two axes correspond to detectors with roughly the same angle θ between them, gating on the first axis for selectivity will (to a good approximation because of the near-isotropy of EUROGAM2) maintain the non-alignment of the top state in a cascade observed on the other axes. Cubes for detectors at different angles θ then allow the determination of the γ–γ directional correlation function. Fig. 4 shows the validity of this approach as applied to cascades of known properties. For the cascades of two stretched electric quadrupoles (E2-E2) on the left-hand side of the figure the theoretical value of the coefficients A_{22}/A_{00} and A_{44}/A_{00} are 0.102 and 0.009 respectively. For the stretched E1-E2 cascades on the right the theoretical values are -0.07 and zero respectively.

5. Polarizations

There is a higher cross section for Compton-scattering of a linearly polarized photon in a direction perpendicular to the plane containing the electric field vector and the momentum vector than there is in a direction parallel to that plane. The construction of the 'clover' detectors in EUROGAM2 , in which four germanium crystals sit side by side forming a square, allows these detectors to be used as Compton polarimeters. The clovers are placed close to 90° to the beam direction and arranged such that scattering from one element to another either corresponds to scattering in the plane defined by the beam axis and the line joining the target to the clover detector, or scattering perpendicular to that plane.

In a γ_1-γ_2 cascade beginning on a state which is equally populated amongst its substates the probability of there being a coincidence event for two detectors with angle θ between them, and with Ψ the angle between the direction of the electric field vector and the plane containing the momentum vectors of the two γ rays, is proportional to [8] the function

$$W(\gamma_2; t_1, t_2, \theta, \Psi) = \sum_{\lambda} \left(A_\lambda(t_1, t_2) P_\lambda(\cos\theta) + A_\lambda^{(p)}(t_1, t_2) P_\lambda^{(2)}(\cos\theta) \cos(2\Psi) \right) , \qquad (1)$$

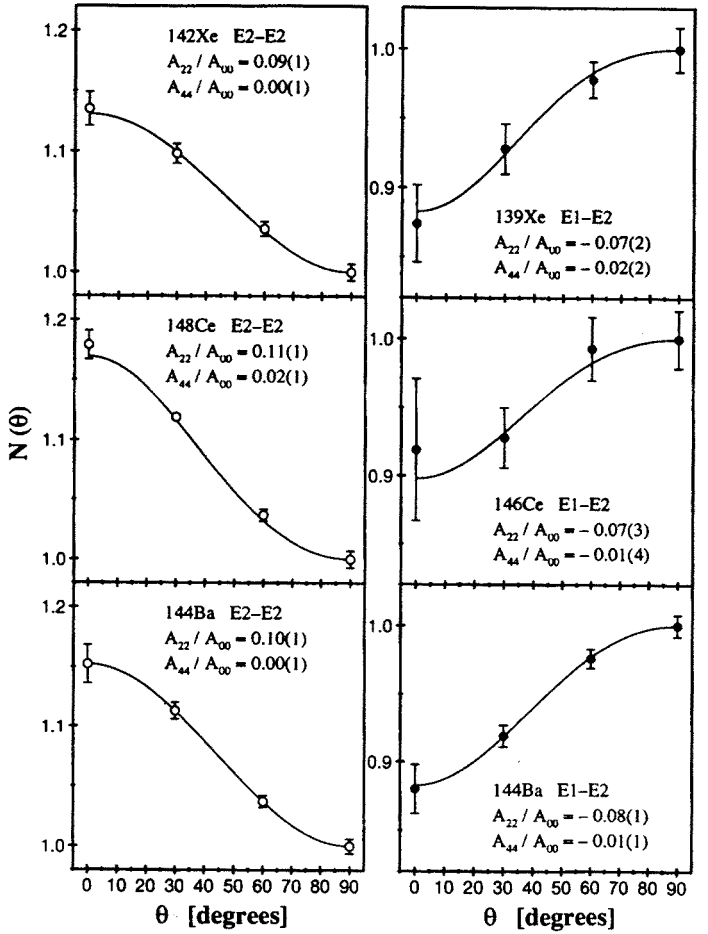

Fig. 4. Observed γ-γ directional correlations for cascades of known type as described in the text, and fits in terms of a distribution function of the form $N(\theta) = A_{00} + A_{22}P_2(\cos\theta) + A_{44}P_4(\cos\theta)$.

where P_λ and $P_\lambda^{(2)}$ are Legendre polynomials and t_1 and t_2 label the properties of the two transitions and the states between which the transitions are made. The coefficients A depend upon the pathways t. If the detection system is insensitive to polarization, integrating over all angles Ψ gives the γ-γ directional correlation function discussed in Section 4.

If data are taken with γ_1 detected in Ge detectors close to zero or 180°, and γ_2 detected via summing scattered signals in two elements of a clover near 90° the situation corresponds to that described earlier. For the angle Ψ equal to zero, the scattering parallel to the plane defined by the momentum

vectors of γ_1 and γ_2 has a lower probability than that perpendicular to the plane, and vice versa if the angle Ψ equals $\pi/2$. The polarization of a beam of γ_2 photons detected in two elements of a clover in coincidence with γ_1 can be defined as

$$P = \frac{W(90,90) - W(90,0)}{W(90,90) + W(90,0)} .$$

Using equation (1) with θ equal to 90°, this can be calculated for given pathways t and depends on the electric and magnetic nature of the transition γ_2. It can be measured by observing the number of scattered events $N_{||}$ and $N_{\perp}$ in appropriate elements of the 'clover' detectors.

$$P = \left(\frac{N_{\perp} - N_{||}}{N_{\perp} + N_{||}}\right)\left(\frac{R+1}{R-1}\right) .$$

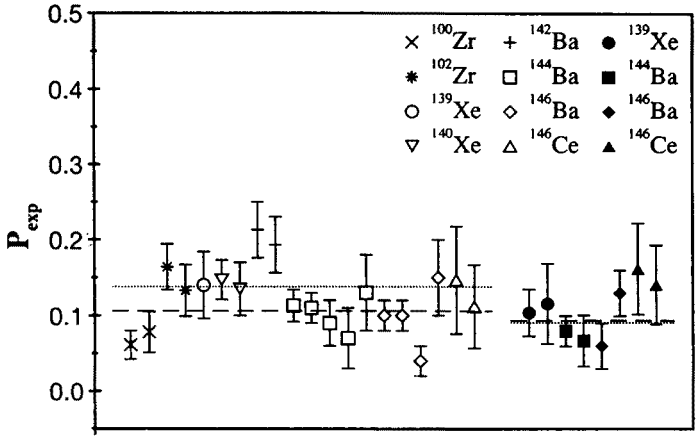

Fig. 5. Observed polarizations P_{exp} for known stretched E2-E2 and stretched E1-E2 γ-γ cascades in strongly populated fission fragments when the angle θ between the two γ rays is in a narrow band around 90°, γ_1 being observed in Ge detectors close to zero or 180°, and γ_2 in clover detectors close to 90°. Filled-in symbols correspond to E1-E2 cascades; open symbols correspond to E2-E2 cascades. The horizontal dashed lines show averages of the two sets; the dotted lines show predicted values.

Comparison of measurement with predictions then gives information on the multipolarity and parity of the transition γ_2. In the above formula R is a parameter depending on the different Compton scattering cross-sections at zero and 90°. For non-point detectors averaging over all angles involved

gives

$$P = \frac{1}{Q} \frac{aN_{\perp} - N_{\parallel}}{aN_{\perp} + N_{\parallel}},$$

where Q is the polarization sensitivity of the polarimeters, obtained by calibration, and a is a factor close to unity which takes into account any instrumental anisotropy.

Fig. 5 shows the validity of the polarization technique as applied to cascades of known properties in various nuclei. In spite of relatively large errors on the data they can still easily distinguish between transitions of pure electric or pure magnetic type because the two P values, although equal, have opposite sign.

6. Lifetimes

For a fission source uniformly embedded in a solid environment the fission fragments to a good approximation are all stopped in a very short time and with ranges of 3–15 mg cm^{-2} depending on the stopping material. The initial energy of a typical fragment from spontaneous fission is about 1 MeV per nucleon, and the range in gold of a fragment of this energy is typically about 13 mg cm^{-2} ($\sim 7 \times 10^{-4}$ cm) with a slowing down time of about 1.5 ps. For a source embedded in a material of lower average atomic number, the rate of energy loss per unit length is lower, the range in mg cm^{-2} somewhat lower and the slowing down time a little longer. If a secondary fragment emits a γ-ray from a state with a lifetime shorter than the slowing down time the energy of the γ-ray is Doppler shifted by an amount depending on the speed of the fragment at the time of emission and the angle of emission of the γ-ray with respect to the direction of motion of the fragment. For γ-rays detected in an array without observation of the fragments the result is a symmetric broadening of the line shapes about energies the γ-rays would have if emitted from fragments at rest. Observation of this broadening, and analyses made assuming knowledge of the slowing down process and of the manner in which the states are produced from the entry points into the secondary fragments have been used [9] to measure lifetimes. The lineshapes must be extracted cleanly enough and the lifetimes must be comparable to the slowing down time for good results to be obtained. Fig. 6 shows an example of fits to yrast transitions in ^{112}Ru.

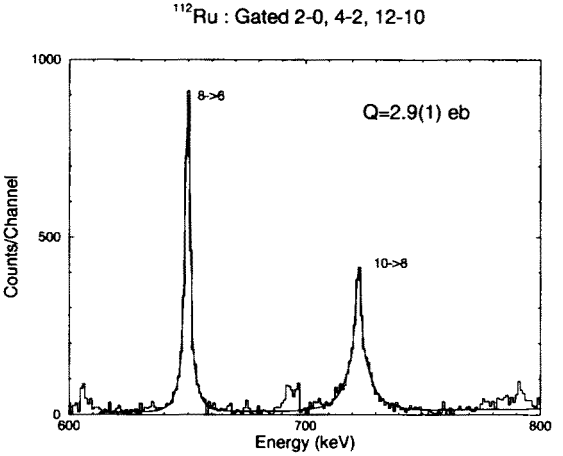

Fig. 6. Fits to lineshape data for yrast transitions in ^{112}Ru using an intrinsic quadrupole moment Q_0 of 2.9 $e$barns.

7. Structures in odd-A lanthanide nuclei–correlation and polarization measurements

The structures at low excitation energy of neutron-rich lanthanide nuclei near $N = 88$ and $Z = 56$ are expected to be influenced by strong octupole correlations because of the ordering and spacing of single-particle orbits near the Fermi surface. Some time ago, features characteristic of octupole deformation or softness in even-even nuclei were found [10, 11], but more conclusive information on the influence of octupole effects can be obtained from studies of odd-A nuclei in this region. In odd-A nuclides, parity doublet bands with similar properties and connected by (usually) strong electric dipole (E1) transitions are expected if the correlations are strong enough to give stable octupole-deformed shapes. Recent experiments on odd-Ba nuclei [12–14] have revealed no strong evidence for such parity doublets although strong E1 transitions were observed [14] using spin-parity assignments based on systematics.

The level schemes of odd-A Ba nuclei have been reinvestigated in order to extend the data and to establish the spins and parities of levels using the correlation and polarization techniques discussed in Sections 4 and 5 and also internal conversion-coefficient measurements. Figs 7 and 8 show partial decay schemes determined [15] for ^{143}Ba and ^{145}Ba by observing prompt γ rays in fragments produced in the SF of ^{248}Cm using the EUROGAM2 array. The data confirm an alternating parity sequence connected by strong E1 transitions in ^{143}Ba. They also reveal a more weakly populated, complementary alternating-parity sequence. The two sequences

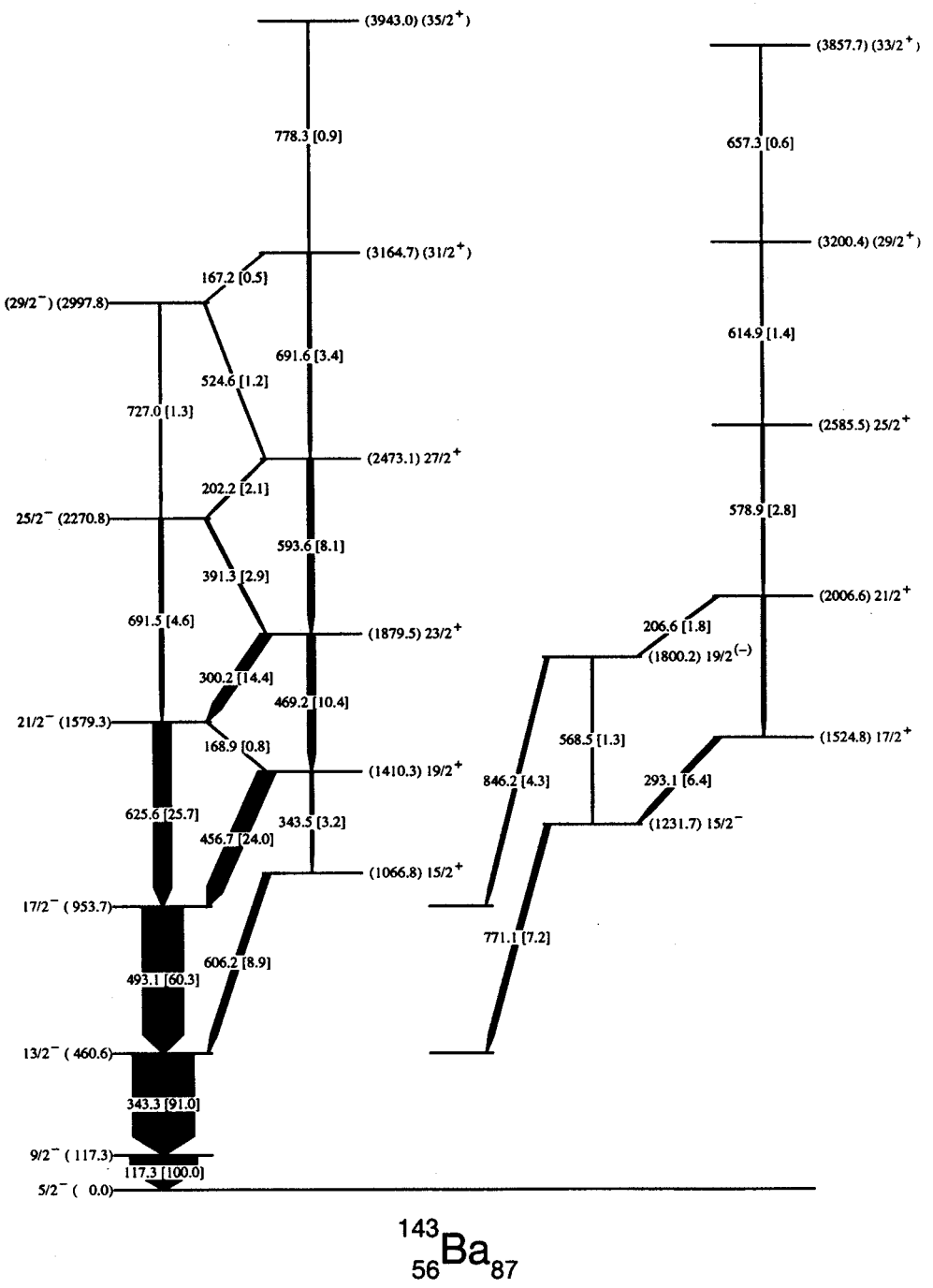

Fig. 7. Partial decay scheme for ^{143}Ba.

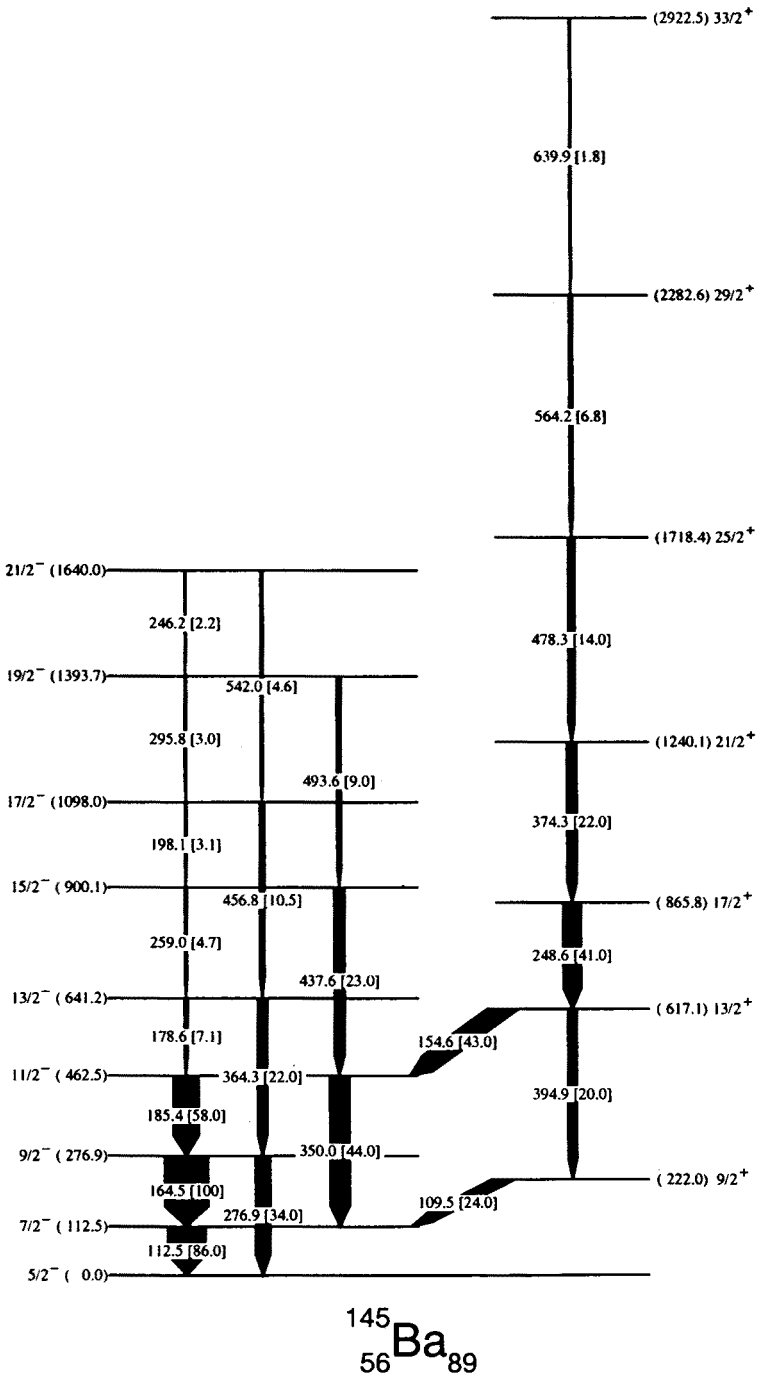

Fig. 8. Partial decay scheme for ^{145}Ba.

together exhibit some properties of parity-doublet bands. Interpreting the E1 strengths in terms of a rotating intrinsic electric dipole moment D_0 by comparison with competing E2 transitions described in terms of a rotating electric quadrupole moment of constant size taken from adjacent even-even nuclei, shows that the size of the E1 moment is similar to those observed in ^{142}Ba and ^{144}Ba. Fig. 9 shows the values of the moment D_0 obtained in ^{143}Ba as a function of spin of level from which the appropriate E1 transition occurred. No well-developed similar structure to that observed in ^{143}Ba is seen in ^{145}Ba, although E1 transitions are observed. Using these to deduce an intrinsic E1 moment produces a value somewhat smaller than that observed in ^{142}Ba. No extended, regular features were observed in ^{147}Ba. A

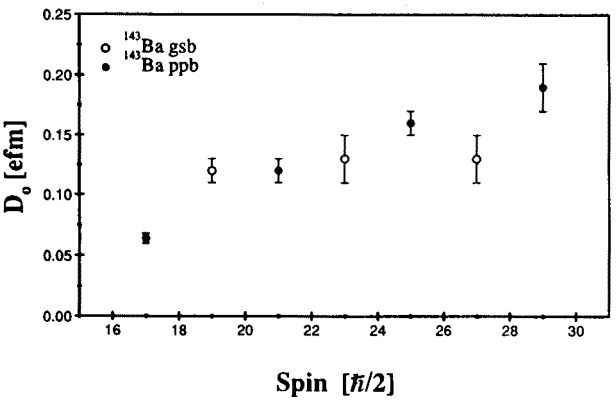

Fig. 9. Values of the intrinsic electric dipole moment D_0 in ^{143}Ba determined within the rotational model. Values are shown against spins of levels from which the competing E1 and E2 transitions originate.

summary of the situation in the odd-A Ba isotopes is that features expected for reflection-asymmetric odd-A nuclei, such as parity-doublet bands, have not been observed in a clearly-developed form, even though the intrinsic electric dipole moments in these nuclei as determined from a rotational model follow the same trend as seen in the even-even isotopes, a trend reproduced by reflection-asymmetric model calculations [16]. In contrast, odd-proton nuclei in this region, such as ^{151}Pm [17] and ^{153}Eu [18], show extended opposite-parity band structures connected by strong E1 transitions. However, these bands exhibit different magnetic properties suggesting a reflection-symmetric rather than asymmetric description. The odd-A La isotopes studied [19] in the EUROGAM2 SF experiments show no clearly defined parity-band structures although the E1 strengths measured determine an intrinsic E1 moment of size similar to those observed in the other odd-Z nuclei. Fig. 10, shows partial decay schemes obtained for ^{145}La and ^{147}La. A reason for the different behaviour observed in odd-N and odd-

Z nuclei in this region may be different blocking effects for neutrons and protons.

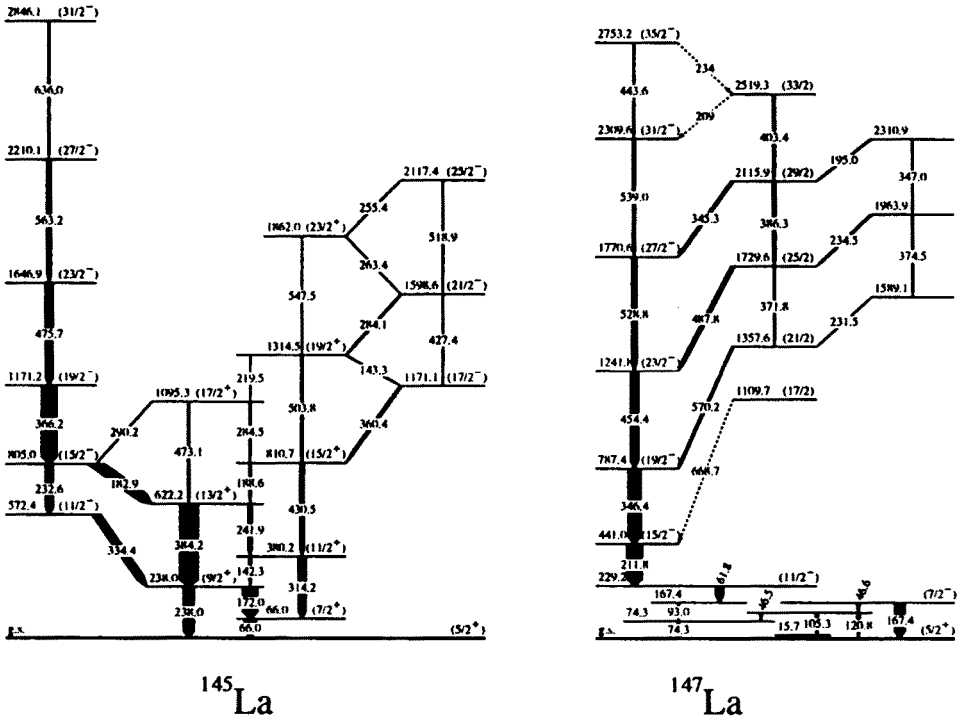

Fig. 10. Partial level schemes for ^{145}La and ^{147}La.

8. Shape trends in the mass 100 region–lifetime measurements

As the neutron number in Sr and Zr isotopes increases through 60 there is a well-known rapid change of ground-state shape to large deformation, with these nuclei exhibiting [6] good rotational features. We have now mea-

sured [20] the lifetimes of higher-lying members of the ground-state bands of ^{98}Sr and ^{100,102,104}Zr, in order to investigate the stability of the deformation with rotation. The measured lifetimes have been transformed into quadrupole moments within a rotational model description. The present results, which correspond to a fit to the lineshapes of γ rays from the decay of the $J = 8$, 10 and 12 members of the ground-state bands, are given in the final column of Table I. The column Raman [21] shows the values of the quadrupole moment derived from the lifetimes of 2^+ states; that labelled Moller [22] shows theoretical predictions of ground-state moments. The units are eb. It can be seen that the new data strongly suggest that the shape of these well-deformed nuclei does not change with angular momentum, at least up to spin 12 $\hbar$. This is consistent with theoretical expectations from calculations of Total Routhian Surfaces (TRS) [22].

TABLE I

Intrinsic quadrupole moments in units of ebarns deduced from lifetimes at low and medium spins in even-even Sr, Zr and Mo isotopes.

Nucleus	Raman	Moller	Present
^{98}Sr	3.12(18)	3.14	3.17(20)
^{100}Zr	3.01(19)	3.36	3.19(10)
^{102}Zr	4.01(40)	3.51	3.52(17)
^{104}Zr		3.68	3.72(16)
^{102}Mo	3.26(19)	3.29	2.44(17)
^{104}Mo	3.29(13)	3.54	2.84(14)
^{106}Mo	3.62(10)	3.70	2.85(13)
^{108}Mo	3.58(42)	3.46	2.79(20)

In contrast to the rigidity of the Sr and Zr isotopes, the Mo isotopes exhibit softness towards triaxiality as spin increases. This is also predicted by TRS calculations which suggest that, as the nuclei rotate, the yrast states take on a triaxial shape, due to the alignment of $h_{\frac{11}{2}}$ neutrons. The role of the γ degree of freedom in the Mo isotopes is of interest, because the Ru isotopes exhibit [23] characteristics of rigid triaxiality. Thus the transition from axial symmetry in the Sr and Zr isotopes to rigid triaxiality in Ru, via the γ-soft Mo isotopes needs further investigation. One consequence of the predicted shape change with rotation in the yrast states of the Mo isotopes would be a change in the quadrupole moment as one moves up the band. We have measured [20] the lifetimes of the $J = 8$ to 12 yrast states in $^{102-108}$Mo and extracted quadrupole moments within a rotational model prescription as before to compare them to the moments determined for the $J = 2$ states. The results are also given in Table I.

It can be seen that, in contrast to the data for the Sr and Zr isotopes, there is a consistent reduction of 20% in the quadrupole moments of the

intermediate spin states in the Mo isotopes. This reduction is in agreement with the theoretical predictions and indicates that there is a change in shape towards a positive non-zero value of γ as the nuclei rotate.

The work discussed in this paper has been performed in collaboration with several researchers from Argonne National Laboratory, USA, and the CNRS Laboratory at Strasbourg. For help with the preparation of this paper special mention should be made of M.A. Jones, J.L.Durell and W.Urban. The work was supported by the Science and Engineering Research Council of the UK under grant no. GRH71161, and by the US Dept. of Energy under contract No. W-31-109-ENG-38. The authors are also indebted for the use of ^{248}Cm to the Office of Basic Energy Sciences, US Dept. of Energy, through the transplutonium element production facilities at the Oak Ridge National Laboratory.

REFERENCES

[1] B.F.Rider, *Vallecitos Nuclear Center Report No. NEDO-12154-3(B)*, 1980
[2] K.F.Flynn *et al.*, *J.Inorg. Chem.* **37** 881-5 (1975)
[3] R.W.Peele and F.C.Maienschein, *Phys. Rev.* **C3** 373-90 (1971)
[4] V.V.Verbinsky *et al.*, *Phys. Rev.* **C7** 1173-85 (1973)
[5] Y.Abdelrahman *et al.*, *Phys. Lett.* **199B** 504-8 (1987)
[6] M.A.C.Hotchkis *et al.*, *Nucl.Phys.* **A530** 111-34 (1991)
[7] I.Ahmad and W.R.Phillips, *Rep. Prog. Phys.* **58** 1415-63 (1995)
[8] R.M.Steffen and K.Alder, in *The Electromagnetic Interaction in Nuclear Spectroscopy*, ed. W.D.Hamilton (North-Holland, 1975)
[9] A.G.Smith *et al.*, *Phys. Rev. Lett.* **73** 2540-2 (1994)
[10] W.R.Phillips *et al.*, *Phys. Rev. Lett.* **57** 3257-9 (1986)
[11] W.R.Phillips *et al.*, *Phys. Lett* **B212** 402-6 (1988)
[12] J.D.Robertson *et al.*, *Phys. Rev.* **C34** 1012-1023 (1986)
[13] J.D.Robertson *et al.*, *Phys. Rev.* **C40** 2804-2822 (1989)
[14] S.J.Zhu *et al.*, *Phys. Lett.* **B357** 273-80 (1995)
[15] M.A.Jones *et al.*, *Nucl. Phys.* **A605** 133-43 (1996)
[16] P.A.Butler and W.Nazarewicz, *Nucl. Phys.* **A533** 249-61 (1991)
[17] W.Urban *et al.*, *Phys. Lett.* **B247** 238-41 (1990)
[18] C.J.Pearson *et al.*, *Phys. Rev.* **C49** 1239-42 (1994)
[19] W.Urban *et al. Phys. Rev.* **C54** 945-8 (1996)
[20] A.G.Smith *et al.*, *Phys. Rev. Lett.* **77** 1711-1714 (1996)
[21] S.Raman *et al.*, *At. Dat. Nucl. Dat. Tables* **36** 1-96 (1987)
[22] P.Moller *et al.*, *At. Dat. Nucl. Dat. Tables* **59** 185-382 (1995)
[23] J.A.Shannon *et al.*, *Phys. Lett.* **B336** 136-40 (1994)